JOURNAL OF SOLID STATE CHEMISTRY 80, 189–194 (1989)

Bismuth Coordinance in Dilute Alloys of the Noncrystalline $Se_{100-x}Bi_x$ System

A. MUÑOZ, F. L. CUMBRERA,* AND R. MARQUEZ

Departamento de Física de la Materia Condensada, Facultad de Física, Ap° 1065, Sevilla, Spain

Received October 12, 1988; in revised form January 30, 1989

The glass transition temperature, T_g, and the coordination peak of the radial distribution function, obtained from electron diffraction experiments, are studied for amorphous thin films of the $Se_{100-x}Bi_x$ system ($x \leq 8$) prepared by vacuum evaporation. The controversial problem of the coordination of Bi in these alloys is raised. The T_g data versus composition are analyzed by means of a simple analytic model. All results can be interpreted by assuming that the average coordination of Bi for the more dilute portions of the system is four, as opposed to the expected value of three, and three when x is greater than 5. © 1989 Academic Press, Inc.

1. Introduction

Whether the electronic properties of amorphous chalcogenide semiconductors can be modified or controlled by addition of impurities or dopants is of great interest. In this way, the effects of various kinds of foreign atoms on some physical properties have been intensively studied, especially for the case of the Se–As system (*1, 2*). The Bi-doped semiconductor exhibits a striking feature: it shows *n*-type conduction (*3–5*), whereas almost all of the noncrystalline chalcogenides show *p*-type conduction and are insensitive to doping of impurities.

On the other hand, the existence of a stable liquid immiscibility in the $Se_{100-x}Bi_x$ system over some part of their phase diagram has been demonstrated (*6–8*). This fact explains the limited number of papers dealing with this system. According to Fleury *et al.* (*9*), above 3 at.% in Bi, their evaporated $Se_{100-x}Bi_x$ samples were no longer amorphous. However, recent thermoanalytical experiments (*7, 8, 10*) suggest the possibility of extending the region in which the system behaves as a homogeneous amorphous solution by suitable control of the conditions of preparation.

Another outstanding problem in amorphous Se–Bi relates to the coordinance of Bi in nonstoichiometric alloys. From previous literature (*11–14*) three coordinations appear as the most likely: three-, four-, and sixfold coordinated Bi. Saiter (*10*), bv means of the study of the structural relaxation of amorphous films of the $Se_{100-x}Bi_x$ system, determined the coordinations to be three and four; particularly, the presence of Bi_4^+ defects could account for the observed inversion in the conduction type.

The purpose of this paper is to bring supplementary insight into the coordinance

* To whom correspondence should be addressed.

0022-4596/89 $3.00

problem by means of two experimental methods, namely

(i) thermoanalytical techniques: by modeling the dependence between the glass transition temperature, T_g, and the average coordination in the binary system; and

(ii) electron-diffraction experiments: starting from the coordination peak of the radial distribution function (RDF).

2. Experimental and Methods

2.1. Sample Preparation

The starting materials for all samples were 5-9's pure Se and Bi (Johnson-Matthey). Thin films of the $Se_{100-x}Bi_x$ system with $x \leq 8$ were prepared by vacuum coevaporation at a residual pressure of 2×10^{-4} Pa from two separate alumina crucibles heated independently. The thickness of the amorphous films were about 50 nm for samples assigned to electron diffraction experiments and about 1.5 μm for those assigned to calorimetric experiments. Glass substrates were used and kept at room temperature during deposition. Samples for electron diffraction were detached from the substrate and transferred to the electron microscope whereas those assigned to calorimetric measurements were scraped off and put into calorimeter sample pans. The thickness and composition of all deposited films were controlled during preparation by means of a quartz microbalance. The final composition of samples containing Bi was determined by the electron microprobe method. The glassy and homogeneous nature of the as-prepared samples was checked by electron diffraction and calorimetric experiments carried out for this purpose. More details of the experimental arrangement were described elsewhere (*8*).

2.2. Differential Scanning Calorimetry

Measurements were made on a Perkin–Elmer DSC-2C scanning calorimeter and a constant scanning rate of 10 K min^{-1} was used. The experiments were performed under pure argon atmosphere. Calibration of temperature was carried out by measuring the transformation curve of melting of pure In and Pb. The temperature scale was calibrated using standards within ±0.2 K. Samples about 3 mg, stripped from the substrate, were placed in crimped aluminum DSC pans. Reaction of the sample with the aluminum pans is negligible up to 775 K.

2.3. Compositional Dependence of T_g

Taking advantage of the previous knowledge (*15*) of the correlations between T_g and structure for polymeric systems, Berkes (*16*) has proposed a simple analytic model for this purpose applicable to inorganic compounds. The basic assumption of the model is that the average coordination in the system is directly related to T_g as

$$T_g = T_g^0 \bar{C}$$

$$\bar{C} = \sum_i C_i X_i,$$

where $\bar{C}$ is the average coordination for covalently bonded materials, and the factor T_g^0 is calculated by assuming that Se added to itself will not change T_g. The variables C_i and X_i are the bonded coordination and the atom or mole fraction, respectively, of the glass-forming species present. Consequently, $T_g^0 = T_g(\text{Se})/2$.

2.4. Electron Diffraction

The structure of liquids and amorphous solids is described by the radial distribution function $\rho(R)$, obtained from the relation

$$4\pi R^2\rho(R) = 4\pi R^2\rho_0 + \frac{2R}{\pi} \int_0^\infty Si(S) \sin(SR)\, dS$$

in which ρ_0 is the mean density of atoms, $S = 4\pi \sin\theta/\lambda$, and the kernel of the integral

$$F(S) = Si(S)$$

is sometimes called the reduced interference function.

In practice, $i(S)$ is calculated directly from the corrected and normalized intensity observable in a diffraction experiment as

$$i(S) = \frac{I_\eta - \langle f^2 \rangle}{\langle f \rangle^2},$$

where I_η is the coherent-scattering intensity in absolute units, $f(S)$ are the scattering factors, and $\langle\ \rangle$ refers to composition averages.

An extensive study about the techniques of diffraction, data reduction processes, and methods for the elimination of spurious errors is reported in the previous literature (see, for example, (*17–19*)). Particularly, the authors have exhaustively studied (*20–22*) the experimental and theoretical strategies to improve the results obtained by means of electron diffraction.

In general, information about the short-range structure can be obtained from the positions and areas beneath maxima in RDF curves: nearest-neighbor spacings, average number of nearest neighbors, and the mean bond angle. This last magnitude γ can be deduced from the radius of the first and second coordination spheres, R_1 and R_2, according to

$$\gamma = 2 \sin^{-1}(R_2/2R_1)$$

since R_2 corresponds to the separation of atoms linked together through their common nearest neighbor.

For the case of a binary amorphous alloy, the area subtended under the first maximum (the coordination peak) is given by

$$A = \int_a^b 4\pi R^2 \rho(R)\, dR = \sum_{\alpha,\beta} \frac{X_\alpha f_\alpha f_\beta}{\langle f \rangle^2} n_{\alpha,\beta},$$

$n_{\alpha,\beta}$ being the mean number of atoms of type β surrounding an atom of type α.

In the present work we used the maximum entropy method (MEM) to obtain the optimum $\rho(R)$ function. Details of the method are described elsewhere (*21–23*).

All electron diffraction experiments were carried out inside a Phillips EM 300 electron microscope operated at 80 kV. The diffraction patterns were recorded photographically on Kodak film and then scanned with a Joyce Loebl-3cs microdensitometer. The photographic calibration was carried out by the Karle method (*24*). In order to obtain the area under the coordination peak free of the usual drawbacks we used the Stetsiv (*25*) method, based on the theoretical relation between the height of the first maximum and the limit value of the module of the scattering vector S_{max}.

3. Results

3.1. DSC Experiments

Figure 1 corresponds to a typical DSC scan showing the glass transition and crystallization phenomena. As sketched in the figure, the departure from the baseline was used as the T_g value.

With regard to the bonded coordinations C_i, as a first approximation the 8-N rule can be used, where N is the number of outer electrons of an atom. However, it is well known (*26, 27*) that for amorphous chalcogenide the foreign atoms cannot be considered individually but rather as making up part of more complex structural units. For

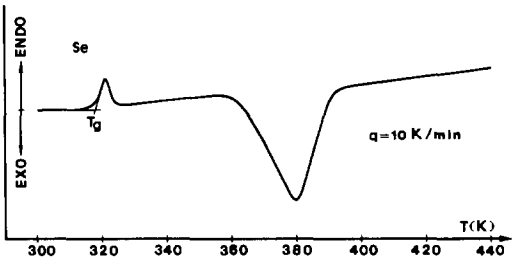

FIG. 1. Typical nonisothermal DSC trace for Se at 10 K min^{-1} heating rate.

example, we consider here the structural groups

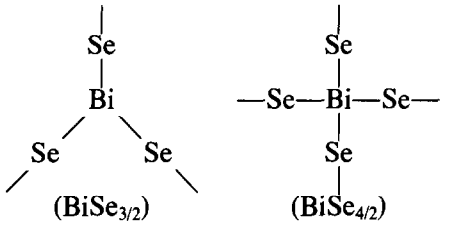

which account, respectively, for the coordinations three and four. In applying this approach for the first assumption we suggest that the material is constructed as a Se–$BiSe_{3/2}$ system composed of Se chains interconnected by the three-coordinated $BiSe_{3/2}$ species. Let ν be the atomic fraction of Bi; consequently, this gives a fraction ν for the $BiSe_{3/2}$ structural unit and a fraction $\{1-\nu-(3/2)\nu\}$ for the Se in the chains. Then, we have

$$\bar{C} = 3\,\frac{\nu}{1-(3/2)\nu} + 2\left[\frac{(1-\nu)-(3/2)\nu}{1-(3/2)\nu}\right] = 2 + \frac{\nu}{1-(3/2)\nu}.$$

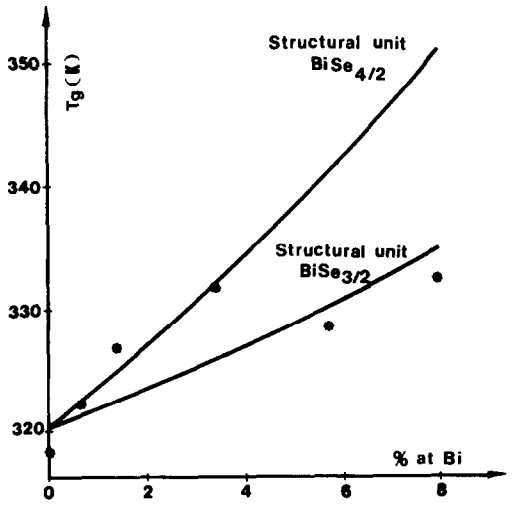

FIG. 2. Experimental (*) and calculated (continuous line) T_g versus Bi content. Two different postulated structural units are contemplated.

TABLE I

T_g VALUES IN THE $Se_{100-x}Bi_x$ SYSTEM AS A FUNCTION OF x

x (% at in Bi)	0	0.7	1.4	3.4	5.7	8.0
T_g (K)	318.2	322.1	327.5	331.5	328.3	332.2

Likewise, we obtain

$$\bar{C} = 2 + 2\,\frac{\nu}{1-2\nu}$$

for the case of $BiSe_{4/2}$ species.

Figure 2 shows the experimental data points of T_g versus Bi content (see also Table I) and the calculated dependence previously analyzed. This figure indicates a trend to the coordination four for Bi contents lower than the 5 at.% and to the coordination three for greater concentrations.

For larger percentages of Bi ($15 < x < 27$), Saiter (*10*) found the formation of $(Bi_2Se_3)_{1-m}Se_m$ clusters, where the Bi is threefold coordinated, freezing the structural relaxation. Such a slow down of the relaxation rate has been likewise observed by one of the authors (*7*) for even lower Bi percentages. This behavior suggests a role for Bi as branching additive connecting neighboring trigonal-like Se chains. The coordination four for Bi may be explained, according to Saiter (*10*), on the basis of the metallic character of this element. Moreover, taking account of the difference in electronegativity between Bi and Se, and according to Fritzche *et al.* (*28*) and Kastner and Fritzche (*29*), it is very likely that Bi behaves as a positive impurity involving, because of electrical neutrality, negatively charged defects (C_1^- for example). The increase in the density of C_1^- defects involves the reduction of the native C_3^+ defects following the reaction $C_1^- + C_3^+ \Rightarrow 2C_2^0$. The disappearance of C_3^+ seems to

be (*10*) closely related to the observed inversion in the type of conduction.

3.2. Electron Diffraction Experiments

The RDF functions of pure Se and those of $x = 2.2$ and $x = 4.3$ are presented in Fig. 3. These RDF functions do not reveal drastic modifications when introducing a slight percentage of Bi in the amorphous selenium matrix. The more prominent change is a continuous and substantial increase with x in the area under the first maximum, despite the low Bi content, which only may be explained by a considerable difference between the coordination two of Se and that of Bi. Table II summarizes the measured and the theoretical (according to the expression reported under Section 2.4) values

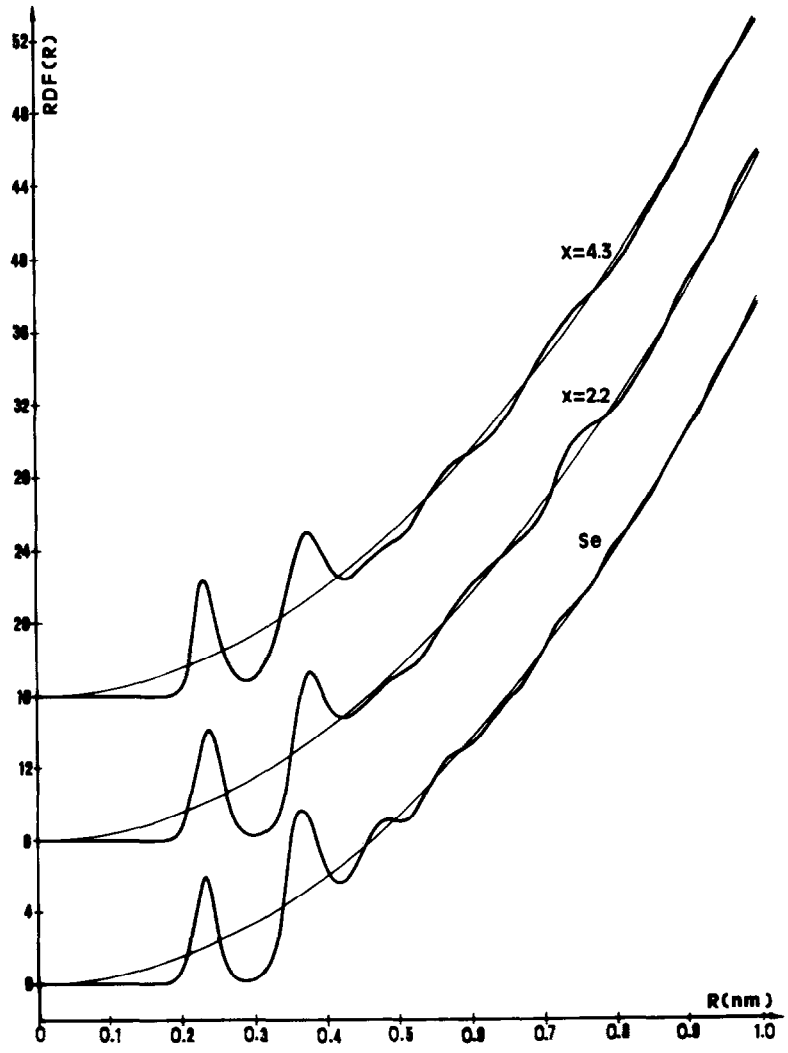

FIG. 3. RDF functions for various compositions obtained by the MEM method.

TABLE II

OBSERVED AREA UNDER THE COORDINATION PEAK OF THE RDF FUNCTION AGAINST THE CALCULATED AREA FOR SEVERAL COMPOSITIONS AND POSSIBLE COORDINATIONS OF Bi

x (% at in Bi)	Observed area	Theoretical area: Postulated Bi coordinance 3	4	6
2.2	2.18	2.08	2.15	2.31
4.3	2.27	2.14	2.30	2.60

of these area for the studied compositions and the possible coordinations of Bi. The results strongly suggest a fourfold coordinated Bi, for this dilute alloy, in agreement with the previous results. Indeed, the calculated value of 0.234 nm for the nearest-neighbor spacing is consistent with the bond length calculated by Vanderbilt and Joannopoulos (*30*) for a superlattice configuration of glassy Se containing C_1^- defects, instead of the expected 0.237 nm for the trigonal Se.

4. Summary

DSC and electron-diffraction experiments were performed on evaporated thin film samples of the $Se_{100-x}Bi_x$ system ($x \leq 8$). On the basis of earlier studies, there is a need to discriminate between the postulated coordination numbers for Bi in this nonstoichiometric alloy. We tried to elucidate this problem for the case of dilute alloys from an experimental point of view. The obtained results are consistent with fourfold coordinated Bi for the lower contents and threefold coordinated Bi for $x > 5$. Particularly, the presence of Bi_4^+ atoms may explain the observed inversion in the conduction type.

References

1. G. PFISTER AND M. MORGAN, *Philos. Mag.* **41,** 209 (1980).
2. M. ABKOWITZ, D. F. POCHAN, AND J. M. POCHAN, *J. Appl. Phys.* **53,** 4173 (1982).
3. H. W. HENKELS AND J. MACZUK, *Phys. Rev.* **24,** 1056 (1953).
4. J. C. SCHOTTMILER, D. L. BOWMAN, AND C. WOOD, *J. Appl. Phys.* **39,** 1663 (1968).
5. N. TOHGE, T. MINAMI, AND M. TANAKA, *J. Non-Cryst. Solids* **37,** 23 (1980).
6. B. MYERS AND J. S. BERKES, *J. Non-Cryst. Solids* **8–10,** 804 (1972).
7. A. MUÑOZ, Doctoral Thesis, Sevilla (1988).
8. A. MUÑOZ AND F. L. CUMBRERA, *Thermochim. Acta,* in press.
9. G. FLEURY, A. HAMOU, C. L'HERMITE, AND C. VIGER, *Phys. Status Solidi A* **83,** K-103 (1984).
10. J. M. SAITER, Doctoral Thesis, Rouen (1986).
11. K. L. BHATTIA, *J. Non-Cryst. Solids* **54,** 173 (1983).
12. T. NAGELS, H. ROTI, AND S. VIKHROV, *J. Phys. C* **4-42,** 907 (1981).
13. N. TOHGE, T. MINAMI, Y. YAMOMOTO, AND M. TANAKA, *J. Appl. Phys.* **51,** 1048 (1980).
14. T. TAKAHASHI, *J. Non-Cryst. Solids* **63,** 413(1984).
15. L. E. NIELSEN, "Mechanical Properties of Polymers and Composites," Vol. 1, Dekker, New York (1974).
16. J. S. BERKES, *J. Non-Cryst. Solids* **25,** 405 (1977).
17. N. J. SHEVCHIK, Ph.D. Thesis, Harvard (1972).
18. R. NARAYAN AND S. RAMASESHAN, *J. Appl. Crystallogr.* **12,** 585 (1979).
19. R. LOVELL, G. R. MIZCHELL, AND A. H. WINDLE, *Acta Crystallogr. Sect. A* **35,** 598 (1979).
20. A. MUÑOZ, F. L. CUMBRERA, AND R. MARQUEZ, *Mater. Lett.* **4,** 262 (1983).
21. A. MUÑOZ, F. L. CUMBRERA, AND R. MARQUEZ, *Mater. Lett.* **7,** 138 (1988).
22. A. MUÑOZ, F. L. CUMBRERA, AND R. MARQUEZ, *J. Mater. Sci.* **23,** 2021 (1988).
23. W. WEI, *J. Non-Cryst. Solids* **81,** 239 (1986).
24. J. KARLE AND I. L. KARLE, *J. Chem. Phys.* **18,** 957 (1950).
25. YA. I. STETSIV, *Sov. Phys. Crystallogr.* **18,** 306 (1973).
26. Z. V. BORISOVA, "Glassy Semiconductors," Plenum, New York (1981).
27. M. B. MYERS AND E. J. FELTY, *Mater. Res. Bull.* **2,** 535 (1967).
28. H. FRITZCHE, P. J. GACZI, AND M. A. KASTNER, *Philos. Mag. B* **37,** 593 (1978).
29. M. KASTNER AND H. FRITZCHE, *Philos. Mag.* **37,** 199 (1978).
30. D. VANDERBILT AND J. D. JOANNOPOULOS, *J. Non-Cryst. Solids* **59–60,** 937 (1983).